Chemical Geology 506 (2019) 29–39

Contents lists available at ScienceDirect

Chemical Geology

journal homepage: www.elsevier.com/locate/chemgeo

Cr isotope systematics in the Connecticut River estuary

Zeyang Sun[a], Xiangli Wang[b,c,*], Noah Planavsky[d]

[a] Department of Geology & Geophysics, Texas A&M University, College Station, TX 77843, USA
[b] Department of Marine Sciences, University of South Alabama, Mobile, AL 36688, USA
[c] Dauphin Island Sea Lab, Dauphin Island, AL 36528, USA
[d] Department of Geology & Geophysics, Yale University, New Haven, CT 06511, USA

ARTICLE INFO

Editor: G. Jerome

Keywords:
Chromium isotopes
The Connecticut River estuary
Riverine Cr flux
Paleoredox proxy
Trace metal

ABSTRACT

Stable chromium (Cr) isotopes (expressed in δ^{53}Cr as the deviation of ^{53}Cr/^{52}Cr in samples from the international standard NIST SRM 979) are an emerging paleoredox proxy that has been used to track Earth's redox evolution over a range of timescales. There have been several major advances in our understanding of the Cr isotope system, but we are still developing a basic knowledge of the global Cr isotope mass balance and there are key Cr fluxes with poorly constrained isotopic compositions. The Cr isotope behavior in estuaries is one such poorly constrained aspect of the modern Cr cycle. Therefore, we collected water and suspended particulate samples from the estuary of the Connecticut River, and present the first Cr isotope dataset from a salinity gradient. As pH and salinity increases from brackish to salt water, dissolved Cr increases from 118.1 ± 25.7 ng/kg (1σ, n = 6) to 225.1 ± 26.0 ng/kg (1σ, n = 8), while particulate Cr decreases from 341.3 ± 319.8 ng/kg (1σ, n = 6) to 208.4 ± 364.5 ng/kg (1σ, n = 8); dissolved δ^{53}Cr decreases from 1.30 ± 0.27‰ (1σ, n = 6) to 0.64 ± 0.16‰ (1σ, n = 8), whereas particulate δ^{53}Cr remained stable at 0.11 ± 0.07‰ (1σ, n = 9). These data suggest that Cr is lost from particles to solution when transitioning from brackish to salt water in the Connecticut River estuary. If these observations can be confirmed in other estuaries, estuary systems can potentially enhance riverine dissolved Cr fluxes and thus lower the Cr oceanic residence time, which has important implications for the Cr isotope system as a paleoceanographic redox proxy. There is a clear inverse correlation between dissolved Cr and δ^{53}Cr in the Connecticut River estuary, which yields a Cr isotope fractionation factor of ~0.89‰ that is indistinguishable from previous estimates based on open seawater samples. Large δ^{53}Cr variation in oxygenated open and estuary seawater suggests that marine δ^{53}Cr variations need not necessarily be exclusively tied to Cr (VI) reduction in low oxygen zones. Therefore, interpreting δ^{53}Cr in the sedimentary record requires taking multiple processes into consideration.

Editor: G. Jerome

1. Introduction

There has been a surge of interest in the past decade in using chromium (Cr) isotopes to track Earth's redox evolution (Frei et al., 2009; Crowe et al., 2013; Cole et al., 2016; Gilleaudeau et al., 2016; Holmden et al., 2016; Wang et al., 2016c; Canfield et al., 2018). Despite pioneering work on Cr isotope geochemistry, we are still working to get a basic sense of Cr isotope behavior on a global scale. There have been several studies on Cr isotope behavior in river systems (Berger and Frei, 2014; Frei et al., 2014; Paulukat et al., 2015; D'Arcy et al., 2016; Wu et al., 2017) and seawater (Bonnand et al., 2013; Frei et al., 2014; Paulukat et al., 2015; Pereira et al., 2015; Scheiderich et al., 2015; D'Arcy et al., 2016; Economou-Eliopoulos et al., 2016; Holmden et al., 2016; Paulukat et al., 2016; Goring-Harford et al., 2018), but there are not yet detailed studies on the Cr isotope behavior in estuaries. Estuaries, where there is mixing of water bodies with widely different physiochemical properties, can dramatically affect river metal fluxes to the oceans (e.g., Boyle et al., 1974). It is debated if, on global scale, Cr behaves conservatively in estuary environments (Cranston and Murray, 1980; Campbell and Yeats, 1984; Abu-Saba and Flegal, 1995). Given that riverine Cr, dominated by particulate Cr, is the major Cr source to oceans, estuaries may play an important role in shaping the global Cr isotope mass balance. For instance, McClain and Maher (2016) suggested that estuaries may reduce the global river Cr flux to the open ocean, and thus increase previously estimated marine Cr residence time. This idea was based on previously observed dissolved Cr

* Corresponding author at: Department of Marine Sciences, University of South Alabama, Mobile, AL 36688, USA.
E-mail address: xwang@southalabama.edu (X. Wang).

https://doi.org/10.1016/j.chemgeo.2018.12.034
Received 1 July 2018; Received in revised form 25 December 2018; Accepted 27 December 2018
Available online 02 January 2019

concentration decreases in estuaries (Cranston and Murray, 1980; Pfeiffer et al., 1982; Campbell and Yeats, 1984; Mayer et al., 1984; Abu-Saba and Flegal, 1995; Frei et al., 2014). However, whether such decrease in dissolved Cr was due to in situ removal processes or simple physical mixing is, in cases, ambiguous.

As a redox-sensitive transition metal, chromium (Cr) has two stable oxidation states in nature, Cr(VI) and Cr(III), with Cr(VI) being much more soluble than Cr(III) under an environmentally relevant pH range (Rai et al., 1989). In modern seawater and river water, Cr(VI) is expected to be the thermodynamically stable form, but significant dissolved Cr(III) is not uncommon (Elderfield, 1970; Jeandel and Minster, 1984), due to complexation with organic ligands (Richard and Bourg, 1991 and references therein), and slow kinetics of Cr(III) oxidation by oxygen in the absence of manganese oxide (Eary and Rai, 1987; Fendorf and Zasoski, 1992).

Rivers are considered the major source of Cr to the ocean, and suboxic and anoxic marine sediments are the major marine Cr sinks (Jeandel and Minster, 1987; Reinhard et al., 2013; Reinhard et al., 2014; McClain and Maher, 2016). Cr in modern seawater is heterogeneous, with concentrations ranging from ~90 to ~340 ng/kg (Bonnand et al., 2013; Paulukat et al., 2015; Pereira et al., 2015; Scheiderich et al., 2015; D'Arcy et al., 2016; Goring-Harford et al., 2018), a much narrower range than existing river water data (58 ng/kg to 1.26 μg/g, five orders of magnitude in range; Berger and Frei, 2014; Frei et al., 2014; Novak et al., 2014; Paulukat et al., 2015; D'Arcy et al., 2016; McClain and Maher, 2016; Wu et al., 2017). The residence time of Cr in the ocean was estimated to be ~9500 years (Reinhard et al., 2013). A new estimate of global river input of Cr is about three times higher than previously thought (McClain and Maher, 2016), suggesting a shorter Cr marine residence time. However, the effects of anthropogenic influences on the riverine Cr concentrations are difficult to gauge. Further, these estimates did not consider the effects of estuaries, which may have large impacts on metal mass balances to the open ocean (e.g., Boyle et al., 1974).

Chromium isotopes have recently been employed as a paleoredox proxy (Frei et al., 2009; Crowe et al., 2013; Planavsky et al., 2014; Cole et al., 2016; Gilleaudeau et al., 2016; Holmden et al., 2016; Wang et al., 2016c), providing an impetus to better constrain modern Cr isotope systematics. Chromium has four stable isotopes: ^{50}Cr, ^{52}Cr, ^{53}Cr and ^{54}Cr, with abundances of 4.35%, 83.79%, 9.50%, and 2.36%, respectively (Rotaru et al., 1992). Chromium redox reactions induce large mass-dependent fractionations (expressed in $\delta^{53}Cr$ as the deviation of $^{53}Cr/^{52}Cr$ in samples from the international standard NIST SRM 979), in which ^{52}Cr preferentially partitions into Cr(III) species, leaving the Cr (VI) enriched in ^{53}Cr (Ellis et al., 2002; Døssing et al., 2011; Kitchen et al., 2012). With limited exceptions (e.g., Schauble et al., 2004; Wang et al., 2015; Saad et al., 2017; Babechuk et al., 2018), non-redox reactions induce negligible Cr isotope fractionation (Ellis et al., 2004; Schauble et al., 2004; Zink et al., 2010; Wang et al., 2015). Therefore, ancient marine sediments can potentially be employed to reconstruct the redox conditions of the ocean-atmosphere system through Earth's history (Frei et al., 2009; Crowe et al., 2013; Planavsky et al., 2014; Gilleaudeau et al., 2016; Holmden et al., 2016; Wang et al., 2016c).

River $\delta^{53}Cr$ appears to be consistently fractionated from the upper continental crust (−0.33‰ −3.9‰; Berger and Frei, 2014; Frei et al., 2014; Novak et al., 2014; Paulukat et al., 2015; D'Arcy et al., 2016; Wu et al., 2017), but there are not yet well constrained estimates for the $\delta^{53}Cr$ value of the globally integrated river flux. Seawater has a much narrower range of $\delta^{53}Cr$ than rivers (+0.31‰ to +1.53‰, Bonnand et al., 2013; Paulukat et al., 2015; Pereira et al., 2015; Scheiderich et al., 2015; Economou-Eliopoulos et al., 2016; Holmden et al., 2016; Goring-Harford et al., 2018). Further, in marine systems there is a strong negative correlation between Cr concentrations and $\delta^{53}Cr$ values, which suggests a global Cr isotopic fractionation factor of ca. -0.8‰ (Scheiderich et al., 2015; Paulukat et al., 2016), in contrast to what has been observed in river systems (Wu et al., 2017). In restricted basins, Cr concentration and $\delta^{53}Cr$ are largely controlled by local factors such as fresh water input, and thus they fall off the correlation line observed for global open seawater (Paulukat et al., 2015).

Compared to rivers and open seawater, estuaries have received relatively little attention, with only seven samples measured for $\delta^{53}Cr$ so far (Frei et al., 2014; Paulukat et al., 2015; D'Arcy et al., 2016), without corresponding salinity data. To better understand Cr isotope systematics in estuarine environments, we collected samples along a pH and salinity gradient in the Connecticut River estuary, and measured Cr concentration and $\delta^{53}Cr$ in both dissolved and suspended loads. We observed systematic changes in Cr concentrations and $\delta^{53}Cr$ along the salinity gradient, which suggests that estuaries may enhance dissolved Cr flux from rivers and smooth out variations in riverine $\delta^{53}Cr$. We also observed an inverse correlation between dissolved Cr concentrations and Cr isotopic compositions, with a comparable fractionation factor to that observed in global open seawater, suggesting a similar mechanism for controlling the fractionation in estuaries and the open oceans.

2. Study region

The Connecticut River is the largest and longest river in New England originating near the U.S. border with Quebec, Canada. It drains a catchment of 4.1×10^{10} m^2 and flows south for ~660 km, across four states (New Hampshire, Vermont, Massachusetts, and Connecticut), and empties into the Long Island Sound (Balcom et al., 2004). It accounts for 70% of freshwater flow into the Long Island Sound (Balcom et al., 2004). Land use of the watershed mainly consists of logging, farming, with limited urbanization and industrialization (Douglas et al., 2002). The lithology of the river basin primarily consists of metasediments, basalt, and glacial sediments (Jahns, 1947; Douglas et al., 2002; Wu et al., 2017). Sediment yields in the Connecticut River are low (7.4×10^9 kg/year, Gordon, 1980), likely linked to recent glacial scouring. There are no major tributaries in the estuary section investigated in this study (Fig. 1).

Freshwater discharge from the Connecticut River into Long Island Sound shows a clear seasonal change, with higher runoff (600–700 m^3/s) during spring than during other seasons (130–160 m^3/s) (USGS, 2003). Connecticut River salinity varies mainly with shifts in freshwater discharge—typically high salinity is associated with low-level runoff during the summer and fall (Garvine, 1974; Garvine, 1975).

Dissolved Cr concentrations in the Connecticut River were previously determined to be 120 ± 60 ng/kg (1σ, n = 16, Wu et al., 2017), which is lower than average global river by an order of magnitude (7790 ± 14,925 ng/kg, 1σ, n = 60, McClain and Maher, 2016), leading to an estimated annual dissolved Cr flux of the Connecticut river into Long Island Sound of 2.1 tons/year (Wu et al., 2017).

3. Materials and Methods

3.1. Samples

In August 2016, we collected 18 water samples from 12 locations (labeled as a-l) along a salinity gradient in the Connecticut River estuary (Fig. 1). At five sampling locations (e, g, i, j, k), samples were collected at different depths. For each sample, approximately 2 L water was collected and stored in 2 L acid-cleaned polyethylene bottles. Within 24 h after sampling, water samples were filtered through 0.2 μm PES membranes (Thermo Scientific Nalgen Rapid-Flow Sterile Filter Units with PES Membrane). The filtered water samples were immediately measured for their salinity and pH, and then stored at 4 °C before chemical analysis and ion exchange chromatography.

3.2. Analytical methods

We separated suspended chromium into two pools: adsorbed Cr and structurally bound Cr. To extract adsorbed Cr, the PES membranes with

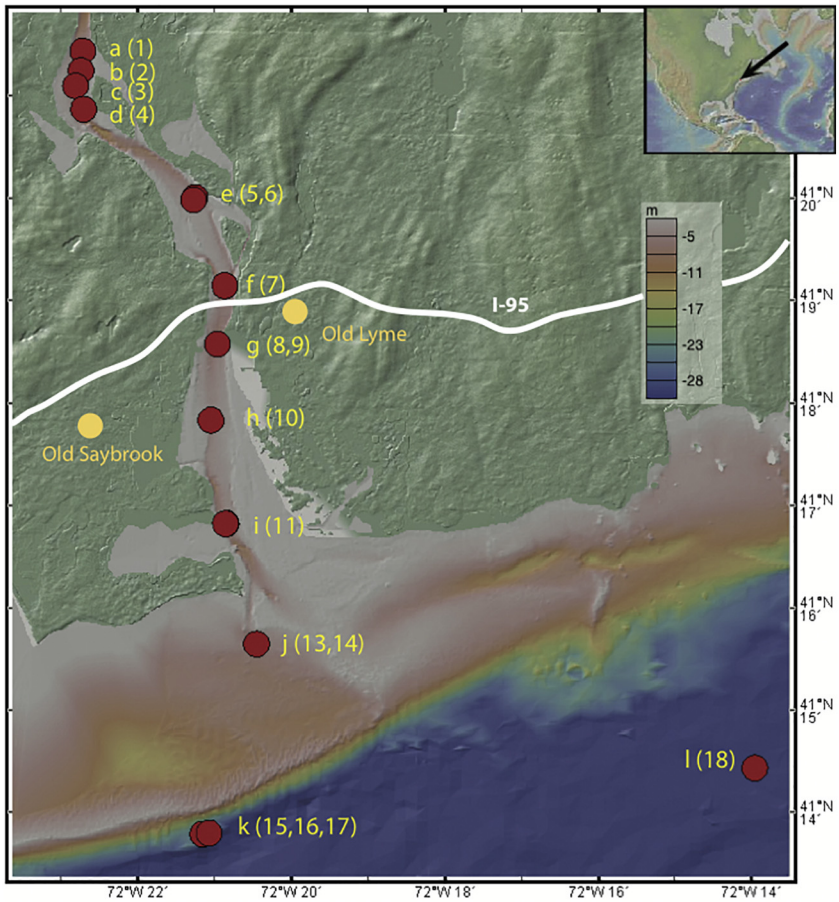

Fig. 1. Sample locations a–l (maroon color) in the Connecticut River and estuary. Numbers in parentheses represent sample number. Color bar represents water depth. (For interpretation of the references to color in this figure legend, the reader is referred to the web version of this article.)

suspended particulate samples were transferred into acid-cleaned 50 mL polypropylene centrifuge tubes, and 35 mL Milli-Q water were added to completely inundate the membranes. After 30 min sonication, membranes were taken out and suspensions were centrifuged for 5 min at 4000 rotations per second. The supernatant was transferred into Teflon beakers, dried down on 130 °C hot plates, treated with aqua regia to destroy organic matter, and eventually dissolved in 4 mL 6 N HCl (labeled with Cr_{ads} to denote adsorbed Cr). To extract Cr structurally bound to particles, the remaining solid materials were completely dissolved with 0.5 mL HCl, 0.5 mL HNO_3 and 0.5 mL HF on 130 °C hot plates for 48 h. Samples were dried down and re-dissolved in 4 mL 6 N HCl (labeled with Cr_{solid} to denote Cr structurally incorporated into particulate matter).

The Cr concentration and $\delta^{53}Cr$ of bulk particulate Cr load (Cr_{part}, ng Cr per kg of water) are calculated as:

$$Cr_{part} = Cr_{ads} + Cr_{solid}$$

$$\delta^{53}Cr_{part} = f \times \delta^{53}Cr_{ads} + (1 - f) \times \delta^{53}Cr_{solid}$$

where f is the fraction of Cr in Cr_{ads} over that in Cr_{part}.

Total Cr concentration is then defined as:

$$Cr_{tot} = Cr_{part} + Cr_{aq}$$

Trace element concentrations for all water samples, Cr_{ads} and Cr_{solid} samples (both in ng Cr per kg water) were measured on a Thermo Scientific Element XR ICP-MS at the Yale Metal Geochemistry Center. An appropriate amount of ^{50}Cr-^{54}Cr double spike, designed to correct for isotope fractionation during sample processing and instrument mass bias (Dodson, 1963; Ellis et al., 2002; Schoenberg et al., 2008), was added to each sample containing ~100 ng Cr based on the measured Cr concentrations. Cr_{ads} and Cr_{solid} samples were then slowly evaporated to dryness, re-dissolved in 0.25 mL 10 N HCl and left with closed lids on a 130 °C hot plate for > 18 h before performing column procedures (below).

Because of the low Cr concentration and high salts in seawater, it is essential to pre-concentrate Cr before performing column procedures to purify Cr. We used the Cr-Fe co-precipitation method (Cranston and Murray, 1978; Connelly et al., 2006) to pre-concentrate Cr from double-spiked ~2 L water samples. After leaving the double-spiked water samples overnight, concentrated ammonium hydroxide (SeaStar) were used to adjust the pH to be 8–9. Fresh ferrous iron oxide was added to samples to reduce Cr(VI) to Cr(III). The precipitated ferric oxyhydroxide uptakes the newly formed Cr(III), together with pre-existing dissolved Cr(III). Therefore, our $\delta^{53}Cr$ measurements are bulk signatures of Cr(III) + Cr(VI). To make fresh ferrous iron oxide, 1 mL of 10% ammonium (1 M) hydroxide (Seastar) was mixed with 50 mL of 0.01 M Fe(II) ammonium sulfate (Sigma Aldrich, 99.99% trace metals basis) dissolved in water. Immediately after creation, 3.5 mL of the 0.1 M fresh Fe(II) hydroxide was added to water samples. After one-hour shaking, the samples were left to stand still overnight, then the majority of clear solution was removed by siphoning. The remaining suspensions (~30–40 mL) were centrifuged to extract the Cr-Fe precipitate, which were then dissolved in 2 mL 6 N HCl.

Fe was removed via anion exchange method (AG1-X8 resin, 100–200 mesh size), and the eluent was completely dried down and re-dissolved in 2 mL vials with 0.25 mL 10 N HCl at 130 °C for over 18 h before Cr purification. All the Cr_{ads}, Cr_{solid} and pre-concentrated seawater samples were processed through the cation exchange chromatography to extract Cr (AG50-X8 resin, 200–400 mesh size; Bonnand et al., 2011). The final eluent was dried down and one drop

Table 1
Sample information.

Sample numbers	Location	Coordinates	Sample depth (m)	Max depth (m)	Temperature (°C)	Salinity (‰)	pH
1	a	41°21.444′–72°22.710′	4	5.24	26.4	9.97	7.23
2	b	41°21.253′–72°22.735′	0	5.24	25.9	6.38	7.16
3	c	41°21.102′–72°22.805′	0	–	26.1	7.96	7.42
4	d	41°20.874′–72°22.698′	0	–	26.3	5.87	7.39
5	e	41°20.017′–72°21.254′	0	4.45	25.3	14.30	7.48
6	e	41°19.993′–72°21.269′	4	4.27	24.5	24.10	7.36
7	f	41°19.153′–72°20.862′	0	6.92	24.1	19.00	7.39
8	g	41°18.580′–72°20.957′	0	8.14	24.1	14.30	7.55
9	g	41°18.580′–72°20.957′	6	8.14	24.1	30.50	7.85
10	h	41°17.839′–72°21.039′	0	4.54	23.9	18.00	7.88
11	i	41°16.826′–72°20.846′	0	6.64	22.2	22.70	7.84
12	i	41°16.826′–72°20.851′	5	6.52	22.2	30.90	7.83
13	j	41°15.648′–72°20.450′	0	6.40	20.7	30.40	7.81
14	j	41°15.648′–72°20.450′	5	6.40	20.7	30.50	7.79
15	k	41°13.785′–72°21.149′	0	25.60	20.1	30.40	7.83
16	k	41°13.785′–72°21.149′	20	25.60	20.1	31.00	7.81
17	k	41°13.801′–72°21.065′	10	23.16	20.7	30.80	7.81
18	I	41°14.436′–72°13.960′	0	–	20.6	30.20	7.86

concentrated HNO_3 was added to remove residual organics leached from the resin. Samples were finally dissolved in 1 mL 0.75 N HNO_3 for isotope analysis. In order to evaluate the accuracy of the Cr-Fe co-precipitation method, 1 L Atlantic seawater (OSIL-) was treated in the same way as water samples, which yielded the same $\delta^{53}Cr$ as previous studies (0.86 ± 0.09‰ and 147.8 ng/kg in this study; 0.96 ± 0.06‰ and 157 ng/kg in Scheiderich et al., 2015; 0.97 ± 0.10‰ and 161.2 ng/kg in Goring-Harford et al., 2018). Total procedural blank Cr ranges from 2 to 4 ng, which is only 2–4% of Cr contained in samples. Cr isotopic values were measured on a Neptune Plus MC-ICP-MS at the Yale Metal Geochemistry center, following procedures described in Wang et al. (2016c). Reproducibility on $\delta^{53}Cr$ during this project is 0.07‰, based on repeated processing and analysis of standard SRM 3112a.

4. Results

Table 1 lists the sample information (location, depth, temperature, salinity and pH values) and Table 2 presents trace element and $\delta^{53}Cr$ data for Cr_{dis}, Cr_{ads}, Cr_{solid}, and Cr_{part}. Combining previous data from the upper stream fresh water (green in Fig. 2, Wu et al., 2017) and data from this study (blue = brackish and maroon = salt in Fig. 2), we observed systematic downstream variations in pH, salinity, $\delta^{53}Cr$, and Cr (Fig. 2). Both pH and salinity increase downstream (Fig. 2A and B), reflecting different extent of mixing between freshwater and seawater. The pH values show a two-step rise, with the first rise from 7.2 to 7.4 occurring from location b to c (blue sample number 2 to 3), and the second rise from 7.4 to 7.8 occurring from location f to h (maroon sample number 7 to 9, Fig. 2A). The salinity exhibits a two-step increase: first rise from 5.87–9.79 to 19–22.4 (brackish) at the transition from location d to e (blue sample number 4 to 6), and the second rise from ~19–22.4 to ~30 (salt) at the transition from location h to i (maroon sample number 10 to 12, Fig. 2B).

$Chromium_{aq}$ remains relatively low in the fresh water section (114 ± 61 ng/kg, 1σ; excluding the most upstream sample), but increases significantly to higher values in the brackish section (236 ± 43 ng/kg, 1σ; Fig. 2C). In contrast, Cr_{part} decreased significantly from the fresh section (913 ± 185 ng/kg, 1σ) to the salt-water section (115 ± 154 ng/kg, 1σ; excluding sample 16 collected near the seafloor). The trend of the Cr_{tot} follows that of the Cr_{part}.

The $\delta^{53}Cr_{aq}$ increases systematically from −0.17‰ in upstream fresh water to 1.71‰ in the end of the brackish water, then abruptly decreases to 0.6–0.7‰ the salt water (Fig. 2D). The abrupt decrease in $\delta^{53}Cr_{aq}$ coincides with the abrupt increase in Cr_{aq}. Such systematic downstream change is not observed in $\delta^{53}Cr_{part}$ (0.09 ± 0.07‰, 1σ).

$\delta^{53}Cr_{aq}$ covaries with water depth and Cr_{aq} but not salinity. At location k in the estuary where we sampled deeper waters down to 20 m, there is a trend of decreasing $\delta^{53}Cr_{aq}$ and increasing Cr_{aq} from surface to deep (Fig. 3A), but increasing $\delta^{53}Cr_{part}$ and increasing Cr_{part} (Fig. 3B). Logarithmic Cr_{aq} and $\delta^{53}Cr_{aq}$ in the Connecticut River estuary are inversely correlated (Fig. 4), and excluding deeper water samples improves the R^2 on linear regression (with exclusion: $\delta^{53}Cr_{aq} = -0.89\ln[Cr_{aq}] + 5.50$, $r^2 = 0.8742$; without exclusion: $\delta^{53}Cr_{aq} = -0.75\ln[Cr_{aq}] + 4.83$, $r^2 = 0.6957$, Fig. 4). Unlike Mo and U that are considered conservative trace metals in the ocean as evidenced by their clear correlations with salinity, Cr_{aq} concentration and $\delta^{53}Cr_{aq}$ are not correlated with salinity (Fig. 5).

As mentioned above we separated the suspended loads into two pools: adsorbed-phase (labeled as Cr_{ads}) and solid-phase (labeled as Cr_{solid}). Cr_{solid}, but not Cr_{ads}, is correlated with corresponding Ti concentrations (Fig. 6A vs. B). However, data for both adsorbed and solid phases plot below the average upper continental crust line (Rudnick and Gao, 2003). In addition, samples from locations a–g (sample number 1 to 9) and locations h–l (sample number 10 to 18) have different slopes in their Cr-Ti plots (Fig. 6B and D). No correlation was found between Cr_{aq} and Cr_{ads} (Fig. 6C). Titanium concentration seems to be higher in the lower estuary than upper estuary, except for location e (sample number 5 and 6) in the intermediate zone (Fig. 2C). The $\delta^{53}Cr_{ads}$ is indistinguishable from $\delta^{53}Cr_{solid}$ (−0.18‰ to 0.36‰). There are no clear correlations between Cr and $\delta^{53}Cr$ values for all adsorbed, solid, and particulate Cr.

5. Discussion

5.1. Low Cr concentration in the Connecticut River

Dissolved chromium concentrations in the Connecticut River and estuary are very low (181 ± 75 ng/kg, 1σ, n = 25; Wu et al., 2017 and this study), compared to other global rivers (7790 ± 14,925 ng/kg, 1σ, n = 60, McClain and Maher, 2016). The low Cr_{aq} concentrations are likely linked to the catchment lithology and the presence of limited anthropogenic influence. Major cation chemistry in the river system suggests that weathering of carbonate rocks, which have low Cr content, has contributed a significant amount of solutes into the river (Douglas et al., 2002). In addition, other sediment types in the catchment system also have very low Cr content in this region (57 ± 24 μg/g, 1σ, Wu et al., 2017) compared to the average continental crust (135 μg/g, Rudnick and Gao, 2003). Although regions of the Connecticut River catchment are populated, there is not a major source of anthropogenic Cr contamination. The lack of downstream increase in

Table 2
Geochemical data for the Connecticut River estuary. Cr_{part}: bulk particulate Cr. DL: detection limit; ND: not determined.

Location	Sample #	Depth (m)	Dissolved							Adsorbed					
			δ^{53}Cr (‰)	2 s.e. (‰)	Cr ng/kg	Mo ng/g	U ng/g	Fe ng/g	Mn ng/g	δ^{53}Cr (‰)	2 s.e. (‰)	Cr ng/kg	Ti ng/g	Fe ng/g	Mn ng/g
a	1	4	1.09	0.04	145.8	3.53	0.91	10.75	17.29	0.16	0.03	87.8	51.1	23.12	0.07
b	2	0	1.18	0.05	138.7	4.09	1.11	11.92	15.93	0.09	0.03	65.8	45.5	25.90	0.10
c	3	0	1.23	0.04	126.1	3.43	0.86	8.34	19.89	0.07	0.02	76.7	45.7	23.06	0.08
d	4	0	1.03	0.03	125.3	2.61	0.58	9.51	21.14	0.11	0.02	74.8	44.9	19.49	0.09
e	5	0	1.55	0.04	84.1	5.74	1.67	4.48	17.08	−0.18	0.02	414.5	292.6	23.89	0.47
e	6	4	1.71	0.05	89.0	10.64	3.22	9.91	8.15	0.19	0.02	564.4	710.6	11.01	0.58
f	7	0	0.47	0.05	236.3	7.47	2.14	6.31	12.31	0.12	0.03	38.5	68.6	18.79	< DL
g	8	0	0.65	0.03	208.8	5.78	1.62	7.57	17.08	0.32	0.05	37.8	38.4	17.64	< DL
g	9	6	0.49	0.10	184.6	11.41	3.20	4.34	5.02	0.08	0.03	48.4	157.8	3.76	0.05
h	10	0	0.51	0.05	266.6	7.33	2.13	6.68	14.16	0.13	0.04	38.1	55.6	15.88	< DL
i	11	0	0.89	0.03	210.9	8.77	2.69	7.59	14.16	0.20	0.05	38.8	59.4	8.87	< DL
i	12	5	0.87	0.04	233.4	11.24	3.16	4.88	3.80	0.23	0.05	50.1	172.3	2.83	0.06
j	13	0	0.63	0.08	211.9	11.87	3.35	5.50	4.09	0.00	0.02	90.9	171.9	6.55	0.10
j	14	5	0.64	0.05	248.1	11.75	3.12	6.10	4.06	0.05	0.03	1064.2	391.0	42.12	1.20
k	15	0	0.98	0.04	198.5	11.42	3.02	4.50	2.62	0.19	0.03	122.4	1082.3	4.71	0.05
k	16	20	0.78	0.04	346.7	11.70	3.39	6.98	0.68	0.36	0.03	566.6	703.4	9.18	0.14
k	17	10	0.86	0.04	270.0	11.73	4.38	4.63	0.59	0.24	0.03	197.1	191.3	33.09	0.62
l	18	0	0.75	0.05	219.6	11.79	3.10	ND	0.47	−0.05	0.03	50.4	73.8	13.89	0.22

Location	Sample #	Depth (m)	Residual solid						Total particulate					
			δ^{53}Cr (‰)	2 s.e. (‰)	Cr ng/kg	Ti ng/g	Fe ng/g	Mn ng/g	δ^{53}Cr (‰)	2 s.e. (‰)	Cr ng/kg	Ti ng/g	Fe ng/g	Mn ng/g
a	1	4	0.29	0.03	47.1	3.6	0.24	0.05	0.20	0.03	134.8	54.7	23.36	0.12
b	2	0	ND	ND	124.4	8.7	0.56	0.11	ND	ND	190.3	54.3	26.46	0.21
c	3	0	−0.07	0.08	45.2	3.3	0.31	0.05	0.02	0.03	121.9	49.0	23.37	0.13
d	4	0	−0.02	0.06	36.6	2.6	0.20	0.04	0.07	0.03	111.4	47.5	19.69	0.13
e	5	0	0.29	0.04	232.4	12.7	0.53	0.24	−0.01	0.02	646.9	305.3	24.42	0.71
e	6	4	0.10	0.04	278.4	27.1	0.87	0.31	0.16	0.02	842.7	737.6	11.88	0.89
f	7	0	ND	ND	14.6	3.2	0.08	< DL	ND	ND	53.1	71.9	18.87	< DL
g	8	0	ND	ND	16.8	2.0	0.13	< DL	ND	ND	54.6	40.4	17.77	< DL
g	9	6	0.25	0.05	33.0	6.5	0.24	< DL	0.15	0.03	81.4	164.3	4	< DL
h	10	0	ND	ND	10.9	2.4	0.09	< DL	ND	ND	48.9	58.0	15.97	< DL
i	11	0	ND	ND	15.5	2.4	0.09	< DL	ND	ND	54.4	61.7	8.96	< DL
i	12	5	0.08	0.06	44.0	10.0	0.34	0.05	0.16	0.04	94.1	182.3	3.17	0.11
j	13	0	0.29	0.05	85.2	17.6	0.51	0.08	0.14	0.03	176.1	189.5	7.06	0.18
j	14	5	0.07	0.05	40.2	7.7	< DL	< DL	0.07	0.03	1104.3	398.7	< DL	< DL
k	15	0	ND	ND	581.3	89.3	0.18	< DL	ND	ND	703.7	1171.6	4.89	< DL
k	16	20	0.03	0.07	2704.9	401.9	1.03	0.17	0.20	0.04	3271.5	1105.2	10.21	0.31
k	17	10	0.01	0.06	320.8	50.9	3.80	0.57	0.10	0.04	518.0	242.2	36.89	1.19
l	18	0	−0.07	0.07	36.9	5.1	2.11	0.38	−0.06	0.03	87.3	78.8	16	0.6

Cr_{tot}/Ti_{tot} (normalization by Ti is to account for varying suspended particle load (Fig. 7) is consistent with limited anthropogenic influence within the studied region.

5.2. Non-conservative Cr in the Connecticut River estuary

There is a debate if Cr behaves largely conservatively in estuary and marine environments on a global scale. In the global ocean, Whitfield (1987) classified Cr as a recycled element (i.e., non-conservative), whereas results from Mugo and Orians (1993) and Sirinawin et al. (2000) suggest that Cr's behavior in the ocean falls between “recycled” and “accumulated” (conservative). In the Columbia River estuary, Cranston and Murray, 1980 observed a negative correlation between Cr_{aq} and salinity, suggesting a simple two-endmember mixing between Columbia River and seawater Cr. They also observed constant $Cr(VI)_{aq}$ across the salinity gradient, suggesting that Cr(VI) is conservative. In contrast, non-linear relationship between Cr_{aq} and salinity in the San Francisco Bay estuary (Abu-Saba and Flegal, 1995) and the St Lawrence River estuary (Campbell and Yeats, 1984) points to complex mechanisms responsible for non-conservative behavior of Cr in estuary environments.

The section of the Connecticut River investigated in this study does not have tributaries. Thus, the non-linear relationship between Cr_{aq} and salinity cannot be explained by different sources with varying Cr concentrations. Temporal variation can also be ruled out because all samples were collected on the same day. Therefore, our data is consistent with the hypothesis that Cr is a non-conservative trace metal in the Connecticut River estuary system (Fig. 5). Linear relationships between Mo and salinity (Fig. 5C), and between U and salinity (Fig. 5D) suggest that simple mixing between river and seawater endmembers are controlling the distribution of these two metals in the estuary. This observation is consistent with the typical view that Mo and U are two of the conservative trace metals in the ocean (e.g., Anbar, 2004; Andersen et al., 2016), albeit with exceptions in some coastal or local reducing waters (Dellwig et al., 2007; Archer and Vance, 2008; Noordmann et al., 2015). In contrast, Cr_{aq} is not correlated with salinity in the Connecticut River estuary (Fig. 5A), suggesting that mechanisms other than simple mixing between seawater and river water are controlling Cr_{aq}. Photochemical redox transformation (Pettine and Millero, 1990; Hug et al., 1996), biological uptake (Pereira et al., 2015; Semeniuk et al., 2016), adsorption/desorption (Richard and Bourg, 1991) are potential factors. Flocculation and colloid aggregation has also been suggested to play an important role in Cr behavior in some estuaries, particularly scavenging $Cr(III)_{aq}$ (Cranston and Murray, 1980; Abu-Saba and Flegal, 1995). Although Cr_{aq} was measured in the filtrate after 0.2 μM filtration, colloid may have passed the filter and thus influence dissolved Cr measurement.

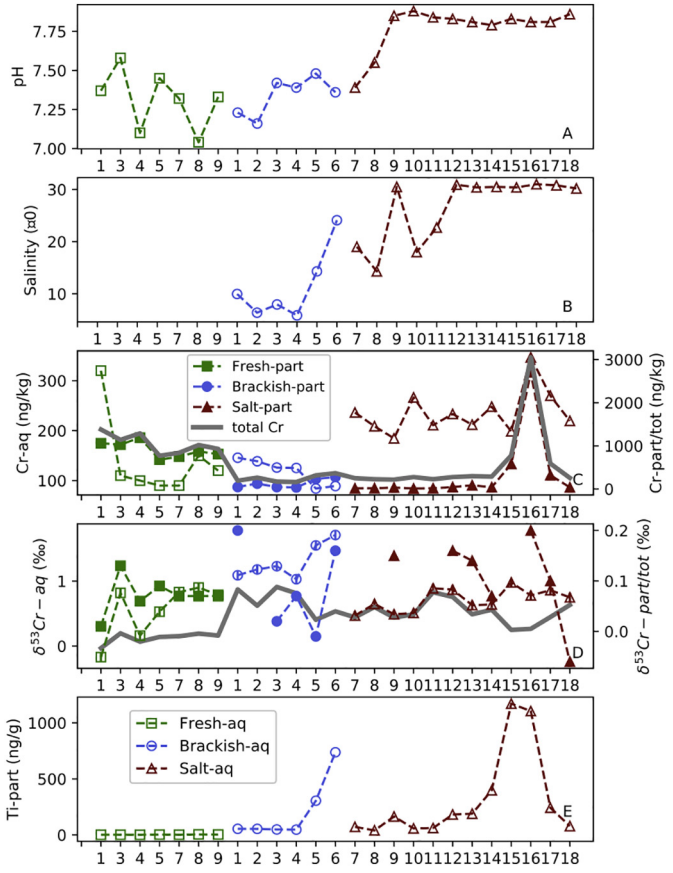

Fig. 2. Downstream trends of pH (A), salinity (B), Cr concentration (C), δ^{53}Cr (D), and Ti (E) in the Connecticut River and its estuary system. Solid and open symbols represent dissolved (aq) and suspended (s). Fresh water (green) data, collected from river surface, are from October samples 1, 3, 4, 5, 7, 8, 9 in Wu et al. (2017). Brackish (blue) and saltwater (maroon) samples are from this study, sampled at locations a-e and f-l, respectively. Samples 1, 6, 9, 12, 14, 16, 17 were sampled from 4 m, 4 m, 6 m, 5 m, 5 m, 20 m, and 10 m, respectively; all other samples were sampled at the surface. All figures share the same legends. (For interpretation of the references to color in this figure legend, the reader is referred to the web version of this article.)

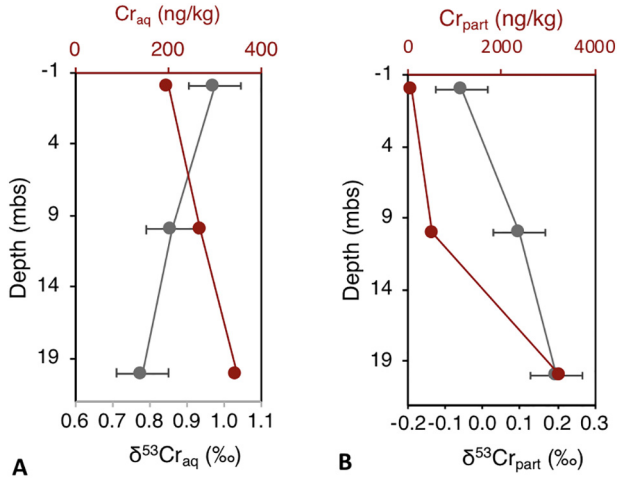

Fig. 3. Depth profile of Cr concentration and δ^{53}Cr at location k from the Connecticut River estuary.

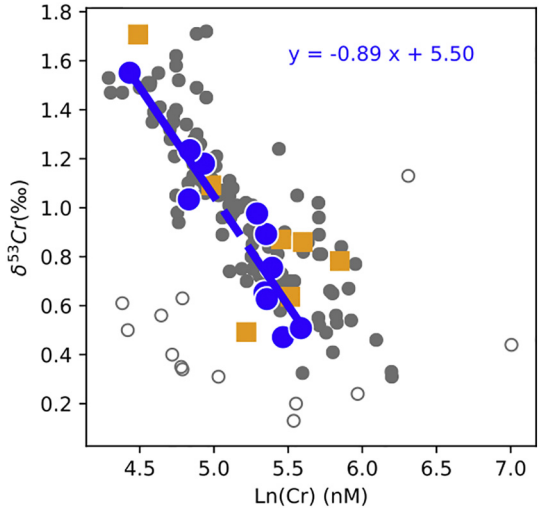

Fig. 4. Inverse correlation between logarithmic Cr concentration and δ^{53}Cr. Colored symbols are from the Connecticut River Estuary (this study). Orange squares are deeper water samples and blue circles are surface water samples. Filled gray symbols represent previous seawater data (Bonnand et al., 2013; Frei et al., 2014; Paulukat et al., 2015; Pereira et al., 2015; Scheiderich et al., 2015; D'Arcy et al., 2016; Economou-Eliopoulos et al., 2016; Holmden et al., 2016; Paulukat et al., 2016; Goring-Harford et al., 2018). Open gray symbols to the lower left are from the Baltic Sea (Paulukat et al., 2016); open gray symbols to the right are estuary samples with extremely high Cr concentration, potentially related to ultramafic and mafic catchment lithology (Frei et al., 2014; Economou-Eliopoulos et al., 2016). Linear regression line and equation are based on surface estuary samples in this study only (blue circles). (For interpretation of the references to color in this figure legend, the reader is referred to the web version of this article.)

5.3. Chromium isotope fractionation

The linear relationship between $\delta^{53}Cr_{aq}$ and natural logarithm of Cr_{aq} of global seawater suggests a uniform Cr isotopic fractionation factor of ~ −0.8‰ (Paulukat et al., 2015; Scheiderich et al., 2015). Using the same approach, we arrive at a Cr isotope fractionation factor of −0.89‰ for the Connecticut River estuary (Fig. 4), which is indistinguishable from previous marine studies (Paulukat et al., 2015; Scheiderich et al., 2015). This suggests that Connecticut River estuary, and perhaps other estuary systems, likely share the same controlling mechanism responsible for Cr removal and attendant isotope fractionation. This is in contrast to rivers, which do not, in the rivers studied thus far, show a correlation between Cr concentration and δ^{53}Cr (Wu et al., 2017).

The exact removal mechanism of Cr from seawater is still debated, although several potential candidates have been mentioned, such as photochemical reduction (Pettine and Millero, 1990; Hug et al., 1996), biological uptake (Pereira et al., 2015; Semeniuk et al., 2016), adsorption (Richard and Bourg, 1991), and colloid formation (Cranston and Murray, 1980; Abu-Saba and Flegal, 1995). The reductive removal of $Cr(VI)_{aq}$, which depends on pH, Eh, and ion chemistry (Accornero et al., 2010), is accompanied by Cr isotopic fractionation, with ^{52}Cr enriched the reduced Cr(III) species and remaining Cr(VI) enriched in ^{53}Cr. Biotic and abiotic Cr(VI) reduction reactions induce Cr isotopic fractionation factors ranging from −0.4‰ to −7.6‰ (e.g. Ellis et al., 2002), which is not incompatible with the one derived from global seawater data and our new estuary data. More species-specific Cr concentration and δ^{53}Cr data are needed to better constrain the Cr removal mechanisms. However, this study clearly demonstrates that fractionation need not be linked to low oxygen conditions.

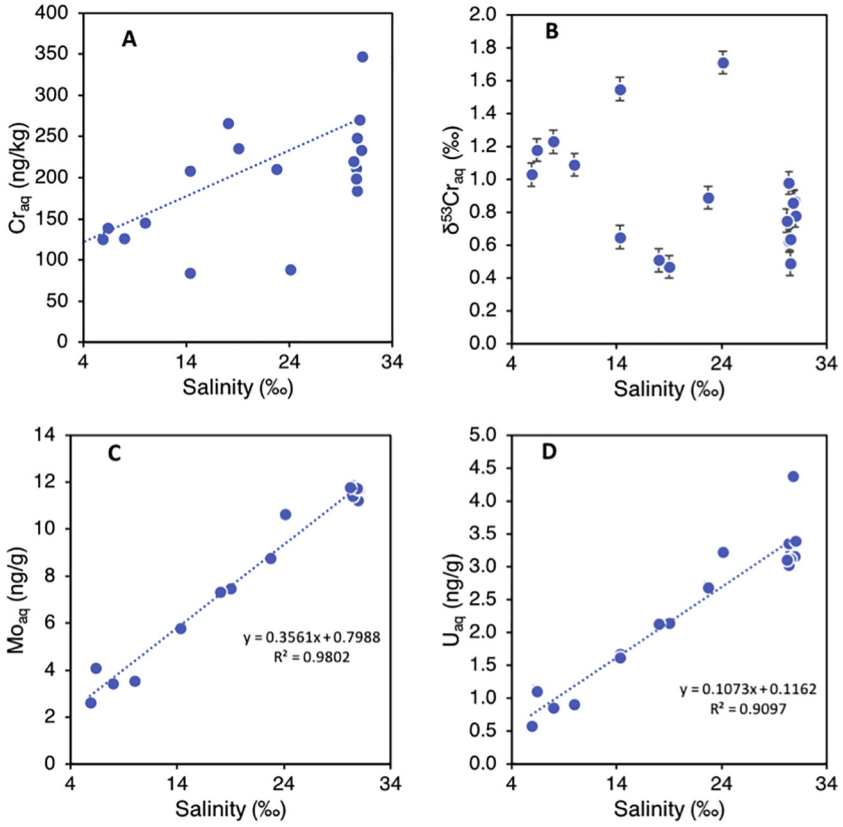

Fig. 5. Cross-plots for Cr_{aq}-salinity (A), $\delta^{53}Cr_{aq}$-salinity (B), Mo_{aq}-salinity (C), and U_{aq}-salinity (D) for the Connecticut River estuary. The dashed line in A is a simple mixing line using river endmember (Cr = 100 ng/kg, Wu et al., 2017; salinity = 0) and Long Island Sound endmember (Cr = 258.7 ng/kg, average of samples 16–18; salinity = 30.7). The dashed lines in C and D are linear regressions. Units are all ng per kg water. Error bars in A and C are smaller than the symbols.

5.4. Depth profile at the mouth of the Connecticut River estuary

Excluding deeper water in our estuary dataset improves the R^2 in the ln[Cr] vs. $\delta^{53}Cr$ plot (Fig. 4), suggesting that there may be other factors affecting deep water Cr and $\delta^{53}Cr$, such as release of Cr from sediments (e.g. Scheiderich et al., 2015). This interpretation is consistent with the observed depth profile of $\delta^{53}Cr$ and Cr concentration at location k (Fig. 3). Relatively high $\delta^{53}Cr_{aq}$ coupled with relatively low Cr_{aq} in surface water (Fig. 3A) is consistent with kinetic isotope fractionation induced by Cr removal. However, such trends in Cr

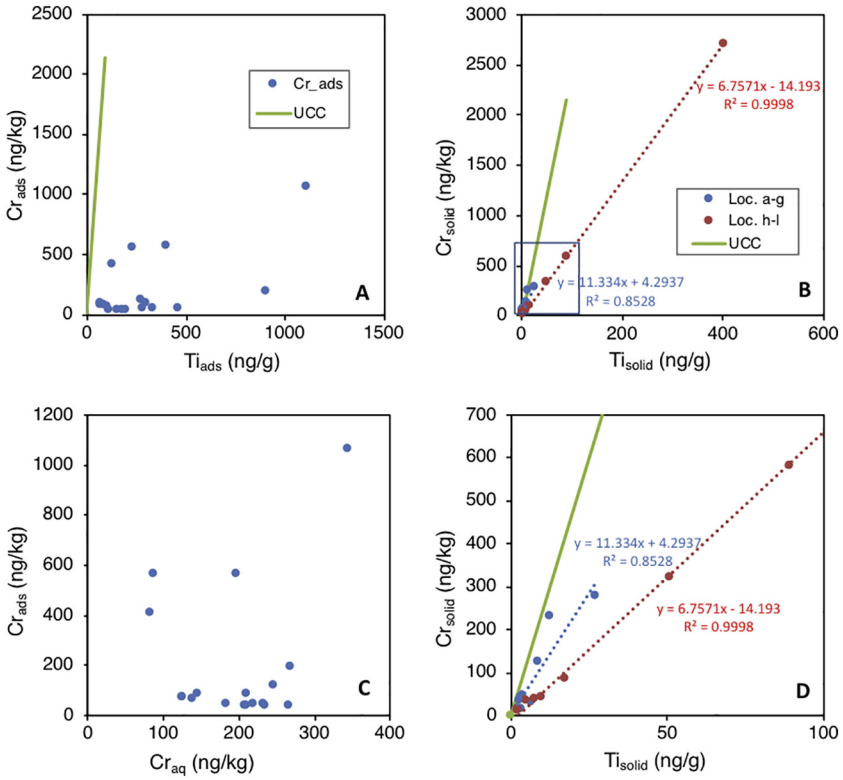

Fig. 6. Cross-plots between Cr and Ti concentrations (A for Cr_{ads}; B and D for Cr_{solid}; D shows details of the rectangle area in B), and between Cr_{dis} and Cr_{ads} (C) in the Connecticut River estuary. Maroon and blue symbols represent data from locations a–g and h–l, respectively. Solid green lines in A, B and D represent the average upper continental crust (Rudnick and Gao, 2003). All units are in ng per kg water. (For interpretation of the references to color in this figure legend, the reader is referred to the web version of this article.)

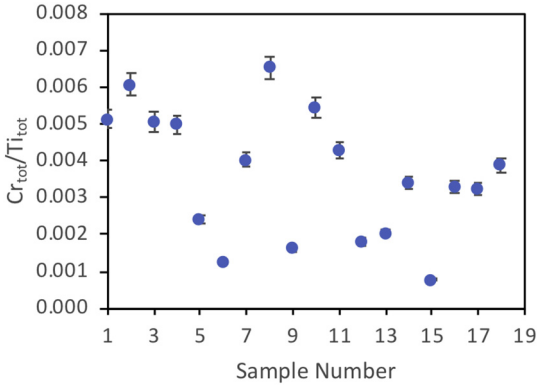

Fig. 7. Total Cr concentration normalized by total Ti concentration along the salinity gradient in the brackish and salt sections of the Connecticut River estuary.

concentration and $\delta^{53}Cr$ are also consistent with diffusion of isotopically light Cr from the bottom, which in turn can be either reoxidized Cr(VI) or organic-complexed Cr(III). These two hypotheses are not mutually exclusive, and can only be differentiated by future species-specific measurement. Reoxidation of Cr(III) near the sediment-water interface has been observed in the Eastern Tropical and Northeastern Pacific Ocean, as well as the Saanich Inlet (Cranston and Murray, 1978; Murray et al., 1983; Rue et al., 1997). Twenty times higher suspended Ti at depth than surface at this location, which has a sediment-water-interface depth of ~20 m, suggests that suspended particles are much higher at deep, likely related to bioturbation or physical sediment reworking, potentially allowing O_2 to penetrate into sediments to oxidize reduced Mn and particle-bound Cr(III).

In contrast to Cr_{aq}, both $\delta^{53}Cr_{part}$ and Cr_{part} increase with depth (Fig. 3B), although $\delta^{53}Cr_{part}$ is much lower than $\delta^{53}Cr_{aq}$ whereas Cr_{part} is an order of magnitude higher than Cr_{aq}. Such isotopically heavy Cr in deep suspended particles can be ascribed to adsorbed Cr(VI), which can be either carried down from the surface or diffusing up from bottom. Regardless of the Cr(VI) origin, the presence of Cr(VI) at deep suggests that the redox condition at the bottom of location k should be oxidizing enough to allow existence of Cr(VI).

5.5. Concentration and $\delta^{53}C$ of suspended particulates

The $\delta^{53}Cr$ values of Cr_{ads} and Cr_{solid} are indistinguishable from each other (Table 2), and both are similar to or slightly above the basaltic-glacial till catchment in this region (Wu et al., 2017), which is within error of the Bulk Silicate Earth, or BSE (-0.1 ± 0.1‰, Schoenberg et al., 2008; Farkaš et al., 2013; Shen et al., 2015; Wang et al., 2016b). There is no correlation between $\delta^{53}Cr_{ads}$ and the $\delta^{53}Cr_{solid}$ (not plotted), suggesting that there was no significant cross-contamination between Cr_{ads} and Cr_{solid}. In contrast to intensively weathered profiles where sub-BSE $\delta^{53}Cr$ has been observed (e.g., Crowe et al., 2013; Berger and Frei, 2014; Frei et al., 2014; D'Arcy et al., 2016), suspended particles (this study and Wu et al., 2017) and marine oxic sediments (Gueguen et al., 2016) do not show sub-BSE $\delta^{53}Cr$ despite variable Cr/Ti ratios. This suggests two possible explanations: 1) there is no significant Cr loss during weathering, and the varying Cr/Ti is due to parent rock heterogeneity (Cole et al., 2017), and 2) weathering loss of Cr from suspended particles during river transport is congruent. The slightly supra-BSE values observed here in the Connecticut River estuary and some marine oxic sediments (Gueguen et al., 2016) are most likely linked to incorporation of $Cr(VI)_{aq}$ from solution.

Sonication washing of suspended particles in this study was designed to rinse off the Cr_{ads}. It was expected that the Cr/Ti ratio of the supernatant should be higher than the average upper continental crust (UCC, Rudnick and Gao, 2003). However, the opposite was observed. Titanium, typically deemed as an insoluble element, was much higher in the sonicated supernatant than the residual solid material (Table 2 and Fig. 6). Although nano molar Ti_{aq} has been observed in deep ocean water (Orians et al., 1990), the median Ti concentration in Cr_{ads} samples (~200 ng Ti per g of seawater) is about three orders of magnitude higher than the highest Ti_{aq} observed in Orians et al. (1990). Therefore, such high Ti in our Cr_{ads} samples is more likely related to nanoparticles remaining in the supernatant after centrifugation. Such potential contamination may be responsible for the lack of correlation between Cr_{ads} and Cr_{aq} (Fig. 6C). However, potential contamination of detrital nanoparticles does not seem to dominate the Cr mass balance in the Cr_{ads}, given the lack of correlation between Cr and Ti (Fig. 6A).

In stark contrast to the adsorbed fraction, the solid fraction has a well-defined linear correlation between Cr and Ti (Fig. 6B and D). Although there is inherent Cr/Ti variability in soil profile samples (Cole et al., 2017), but the Cr/Ti in Connecticut top soils (top 5 cm) is 0.021 ± 0.007 (1σ, n = 9, data from Smith et al., 2014), which is similar to the average UCC. Therefore, the fact that the residual solid material after sonication has lower Cr/Ti than the UCC suggests loss of Cr during weathering and transport. In addition, there seems to be a grouping in terms of Cr_{solid}-Ti_{solid} correlation. The first group (locations a–g, sample number 1 to 10) has a steeper slope than the second group (locations h–l, sample number 11–18) (Fig. 6D). The higher Cr/Ti_{solid} in upstream samples than downstream samples suggests more authigenic Cr in the upper stream samples. Alternatively, different sources of particulate matter with varying Cr/Ti could also explain the difference between upper stream and lower stream particulates.

5.6. Downstream trends in the Connecticut River and estuary

Dissolved $\delta^{53}Cr$ values increase systematically from fresh water into the brackish water (salinity < 10 ppt), then decrease in the mid reach of the estuary (solid symbols in Fig. 2D). In the upstream freshwater portion of the Connecticut River, Wu et al. (2017) attributed the systematic downstream increase in $\delta^{53}Cr_{aq}$ to source rock composition. The fact that the trend of $\delta^{53}Cr_{part}$ follows that of $\delta^{53}Cr_{aq}$ supports this interpretation (Fig. 2D), but a shift in weathering regimes cannot be ruled out. In the brackish region, as the $\delta^{53}Cr_{aq}$ continues to rise, Cr_{aq} decreases (Fig. 2C and D). The negative correlation between Cr_{aq} and $\delta^{53}Cr_{aq}$ suggest that, in this brackish section, Cr_{aq} is removed from solution and is accompanied by systematic Cr isotope fractionation. At the transition from brackish to saltwater, however, $\delta^{53}Cr_{aq}$ decrease abruptly and is accompanied by abrupt increase in Cr_{aq} (Fig. 2C and D). Exceptions to this general trend are a few suspended samples with very high Cr concentrations (Fig. 2C) and Ti concentrations (Fig. 2E). These samples are deeper, and therefore could have been impacted by benthic sediment reworking (Abu-Saba and Flegal, 1995). Such increase in

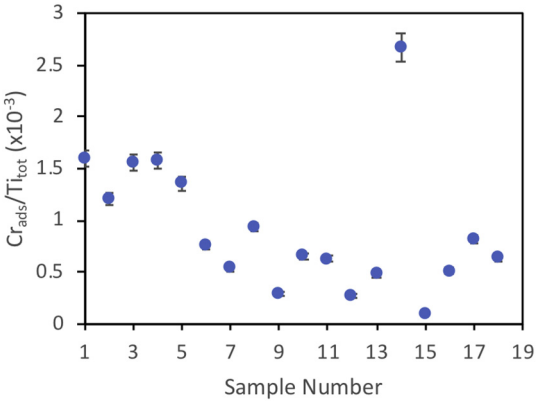

Fig. 8. Decrease of Cr_{aq}:Ti_{aq} ratio from brackish to salt water suggests loss of Cr from particles as water travels downstream in the brackish and salt sections of the Connecticut River estuary.

Table 3
Seasonal chromium fluxes in the fresh, brackish, and salt sections of the Connecticut River. Freshwater data are from Wu et al. (2017). Discharge data are from USGS (2003). Fresh water discharge data are from station 01190070 in the Hartford County, brackish and salt water discharges are from station 01193050 in the Middlesex County. Brackish and salt concentrations represent the averages of samples from locations a–e and f–j, respectively. Samples from locations k–i are excluded because they are part of the Long Island Sound, and thus do not contribute to Cr fluxes from the river.

	Discharge	Cr_{aq}	Cr_{part}	f_{aq}	f_{part}	f_{aq}/discharge	f_{part}/discharge
	m_3/s	ng/kg	ng/kg	ton/year	ton/year	×1000	×1000
Fresh-April	659.8	98.5	1086.3	2.0	22.6	3.1	34.3
Fresh-October	132.2	139.3	753.6	0.6	3.1	4.4	23.8
Brackish-August	162.3	118.1	341.3	0.6	1.7	3.7	10.8
Salt-August	162.3	225.1	208.4	1.2	1.1	7.1	6.6

dissolved Cr partly comes from suspended particles, as suggested by the general decreasing Cr_{ads}/Ti_{tot} trend (Fig. 8). As noted above, Ti can in most cases, be used as a reliable tracer of detrital material, with exceptions in slow-growing metal-rich sediments (Cole et al., 2018). In fact, Ti concentration generally increases downstream (Fig. 2E), suggesting that the Cr_{part} decrease is not due to decrease of suspended particle load, but due to loss of Cr from particles. The mechanism of Cr loss from particle could be either desorption of Cr(VI) or dissolution of Cr(III). Dissolved $\delta^{53}Cr$ suggests the latter, because adsorption should not cause significant change in $\delta^{53}Cr_{aq}$ (Ellis et al., 2004) and ligand mediated dissolution of Cr(III) has been found to induce significant Cr isotope fractionations (Saad et al., 2017; Babechuk et al., 2018). Therefore, large decrease in $\delta^{53}Cr_{aq}$ and increase in Cr_{aq} are consistent with adding detrital Cr from suspended particles.

5.7. Seasonal Cr fluxes in the Connecticut River and its estuary

The effects of the Connecticut River estuary on Cr fluxes to the Long Island Sound can be evaluated by Cr concentration data in the fresh, brackish and saltwater sections. Wu et al. (2017) sampled the freshwater in April and October 2016, whereas this study sampled the brackish and salt water in August 2016. Since river water discharges are similar between August and October (Table 3, USGS, 2003), comparing fluxes from these two months can likely shed some light on the spatial variation along the flow path on the one hand. On the other hand, comparing April and August/October Cr fluxes may reveal seasonal variations in Cr fluxes in the fresh water section, but additional seasonal work is needed.

Chromium flux data are summarized in Table 3. Spatially, brackish f_{aq} (0.6 ton/year) is the same as fresh f_{aq}, whereas brackish f_{part} (1.7 ton/year) is only 50% of fresh f_{part}, (3.1 ton/year). Brackish f_{tot} (f_{aq} + f_{part}, 2.3 ton/year) is 57% of fresh f_{tot} (3.7 ton/year). These observations suggest that Cr_{part} is lost to riverbed over the flow path from fresh to salt sections. Salt f_{aq} (1.2 ton/year) is twice as high as brackish f_{aq}, whereas salt f_{part} (1.1 ton/year) is only 65% of brackish f_{part}. However, salt f_{tot} is the same as brackish f_{tot} (2.3 ton/year). These observations strongly suggest loss of Cr from suspended particles.

Large seasonal variation in Cr fluxes can be concluded using available freshwater data from Wu et al. (2017). April f_{aq} is three times as high as October f_{aq}, whereas April f_{part} is 7 times as high as October f_{part} (Table 3). Higher Cr flux in the spring season is likely related to high river discharge derived from melting snow, which likely flushes soil solutes accumulated over the winter into the river.

Even though f_{part} decreases downstream, in the salt section it still accounts for half of the total Cr flux, consistent with literature data arguing for the importance of suspended particles in river Cr fluxes (Gibbs, 1977; Pettine et al., 1992; Kotaś and Stasicka, 2000). Therefore, owing to its low $\delta^{53}Cr$ and significant Cr flux, the suspended Cr load can potentially influence local seawater $\delta^{53}Cr$ if significant portion of the Cr becomes solubilized.

5.8. Implications for Cr as the paleoredox proxy and mass balance

Current estimates of dissolved Cr flux into the ocean through rivers range from 7.5×10^8 mol/yr to 1.7×10^9 mol/yr (Jeandel and Minster, 1984; Reinhard et al., 2013; McClain and Maher, 2016). Chromium cycling in estuary systems may explain the large range in previously estimated Cr fluxes. Our data suggest that some estuaries can potentially elevate dissolved Cr fluxes to oceans through releasing Cr from suspended particles. Higher riverine Cr flux to the global ocean has significant implications for Cr as a paleoceanographic proxy, because it opens up the possibility that the residence time could be lower than previous estimates based on riverine Cr flux (without considering effects of estuaries). Another estuary system that has positive correlation between Cr_{aq} and salinity is the Beaulieu River that flows into Southampton Water (Dolamore-Frank, 1984). However, in contrast, other studies on Cr concentration and speciation seem to suggest that dissolved Cr can be lost onto particles in the mixing zone within estuaries (Cranston and Murray, 1980; Pfeiffer et al., 1982; Campbell and Yeats, 1984; Mayer et al., 1984; Abu-Saba and Flegal, 1995; Frei et al., 2014). Considering that Connecticut River and Beaulieu River have relatively small dissolved Cr fluxes compared to other major rivers, more data need to be collected to better understand the effect of estuaries on river Cr flux to the global ocean.

Available data show that rivers have a larger range in $\delta^{53}Cr$ (−0.33‰ to 3.9‰, Berger and Frei, 2014; Frei et al., 2014; Novak et al., 2014; Paulukat et al., 2015; D'Arcy et al., 2016; Wu et al., 2017) than seawater (+0.31‰ to +1.53‰, Bonnand et al., 2013; Paulukat et al., 2015; Pereira et al., 2015; Scheiderich et al., 2015; Economou-Eliopoulos et al., 2016; Holmden et al., 2016; Goring-Harford et al., 2018). In this study, the $\delta^{53}Cr_{aq}$ in the Connecticut River estuary ranges from 0.47‰ to 0.98‰ (locations f–l where salinity are relatively high), which is again much narrower than upstream fresh water values

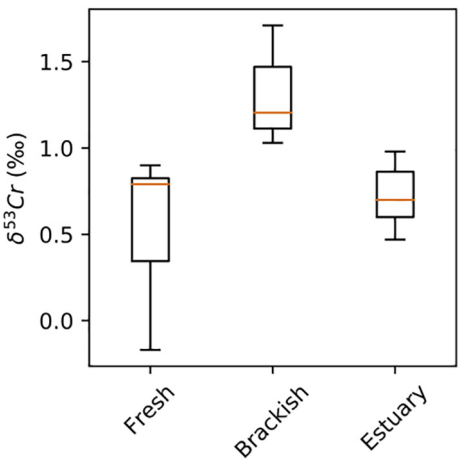

Fig. 9. Boxplot showing decreasing range of $\delta^{53}Cr$ variation from fresh to brackish to salt water.

(−0.17‰ to 0.92‰; Wu et al., 2017) and brackish water values (1.03‰ to 1.71‰ at locations a–e where salinity are relatively high) (Fig. 7). Based on these observations, we tentatively suggest that estuaries can potentially smooth out the $\delta^{53}Cr$ variation of river Cr input (Fig. 9), simplifying one assumption regarding the input term in the global Cr isotope mass balance, in theory, making sedimentary Cr isotope record more straightforward to interpret. However, this idea will need to be verified in other estuaries.

The observation that the fractionation factor in the Connecticut River estuary matches with open seawater from other global locations appears to support a global fractionation mechanism in coastal and open ocean (Scheiderich et al., 2015). On the other hand, large Cr isotope variation in non-reducing waters observed so far does not support a straightforward application of Cr isotope system to tracking redox cycling. Biological activities can alter the conservative vs. non-conservative nature of Cr (compare Cr vs. salinity relationships between Arctic and temperate waters; Scheiderich et al., 2015; this study), and may therefore induce large and variable Cr isotope fractionations (Pereira et al., 2015; Wang et al., 2016a). Therefore, both biological metal uptake and redox processes should be considered when interpreting Cr isotopic compositions of sedimentary rocks in order to infer the expansion or contraction of reducing waters in a largely oxic ocean. This however, does not challenge the idea that the Cr isotope systems can be used to qualitatively track the transition from vastly anoxic Earth system, as generation of soluble Cr(VI) from insoluble Cr(III)–– which requires relatively high level of free O_2–is required to create fractionated $\delta^{53}Cr$ in natural samples (c.f. Frei et al., 2009).

6. Conclusions

This study provides the first comprehensive $\delta^{53}Cr$ and Cr concentration data in dissolved and suspended loads in the Connecticut River estuary, along a salinity gradient. The following conclusions can be drawn: (1) Data from the Connecticut River across a fresh-brackish-salt water gradient suggests that total Cr is partially lost to bottom sediments during transport from fresh to brackish water, and suspended particles appears to lose Cr to solution during transport from brackish to saltwater. Therefore, if future estuarine studies confirm this finding, riverine dissolved Cr flux to the ocean may be larger than previous estimates based on river water, which may reduce oceanic Cr residence time. (2) Chromium behaves non-conservatively in the Connecticut River estuary, with specific controlling factors yet to be identified. (3) There is a clear inverse correlation between Cr_{aq} and $\delta^{53}Cr_{aq}$ in the Connecticut River estuary, which yields a Cr isotope fractionation factor of ~0.89‰ that is indistinguishable from previous estimates based on open seawater samples. (4) Large $\delta^{53}Cr$ variation in oxygenated open and estuary seawater suggests that marine $\delta^{53}Cr$ variations need not be tied to Cr(VI) reduction in low oxygen zones. Therefore, interpreting $\delta^{53}Cr$ in the sedimentary record requires taking into consideration of multiple processes.

Acknowledgement

This work was supported by the Agouron Institute Postdoctoral Fellowship Program, and the National Aeronautics and Space Administration (NASA) Exobiology Program.

References

Abu-Saba, K.E., Flegal, A.R., 1995. Chromium in San Francisco Bay: superposition of geochemical processes causes complex spatial distributions of redox species. Mar. Chem. 49, 189–199.

Accornero, M., Marini, L., Lelli, M., 2010. Prediction of the thermodynamic properties of metal–chromate aqueous complexes to high temperatures and pressures and implications for the speciation of hexavalent chromium in some natural waters. Appl. Geochem. 25, 242–260.

Anbar, A.D., 2004. Molybdenum stable isotopes: observations, interpretations and directions. Rev. Mineral. Geochem. 55, 429–454.

Andersen, M.B., Vance, D., Morford, J.L., Bura-Nakić, E., Breitenbach, S.F.M., Och, L., 2016. Closing in on the marine $^{238}U/^{235}U$ budget. Chem. Geol. 420, 11–22.

Archer, C., Vance, D., 2008. The isotopic signature of the global riverine molybdenum flux and anoxia in the ancient oceans. Nat. Geosci. 1, 597.

Babechuk, M.G., Kleinhanns, I.C., Reitter, E., Schoenberg, R., 2018. Kinetic stable Cr isotopic fractionation between aqueous Cr (III)-Cl-H2O complexes at 25 °C: implications for Cr (III) mobility and isotopic variations in modern and ancient natural systems. Geochim. Cosmochim. Acta 222, 383–405.

Balcom, P.H., Fitzgerald, W.F., Vandal, G.M., Lamborg, C.H., Rolfhus, K.R., Langer, C.S., Hammerschmidt, C.R., 2004. Mercury sources and cycling in the Connecticut River and Long Island Sound. Mar. Chem. 90, 53–74.

Berger, A., Frei, R., 2014. The fate of chromium during tropical weathering: a laterite profile from Central Madagascar. Geoderma 213, 521–532.

Bonnand, P., Parkinson, I.J., James, R.H., Karjalainen, A.-M., Fehr, M.A., 2011. Accurate and precise determination of stable Cr isotope compositions in carbonates by double spike MC-ICP-MS. J. Anal. At. Spectrom. 26, 528–535.

Bonnand, P., James, R., Parkinson, I., Connelly, D., Fairchild, I., 2013. The chromium isotopic composition of seawater and marine carbonates. Earth Planet. Sci. Lett. 382, 10–20.

Boyle, E., Collier, R., Dengler, A., Edmond, J., Ng, A., Stallard, R., 1974. On the chemical mass-balance in estuaries. Geochim. Cosmochim. Acta 38, 1719–1728.

Campbell, J.A., Yeats, P.A., 1984. Dissolved chromium in the St. Lawrence estuary. Estuar. Coast. Shelf Sci. 19, 513–522.

Canfield, D.E., Zhang, S., Frank, A.B., Wang, X., Wang, H., Su, J., Ye, Y., Frei, R., 2018. Highly fractionated chromium isotopes in Mesoproterozoic-aged shales and atmospheric oxygen. Nat. Commun. 9, 2871.

Cole, D.B., Reinhard, C.T., Wang, X., Gueguen, B., Halverson, G.P., Gibson, T., Hodgskiss, M.S., McKenzie, N.R., Lyons, T.W., Planavsky, N.J., 2016. A shale-hosted Cr isotope record of low atmospheric oxygen during the Proterozoic. Geology G37787.1.

Cole, D.B., Zhang, S., Planavsky, N.J., 2017. A new estimate of detrital redox-sensitive metal concentrations and variability in fluxes to marine sediments. Geochim. Cosmochim. Acta 215, 337–353.

Cole, D.B., O'Connell, B., Planavsky, N.J., 2018. Authigenic chromium enrichments in Proterozoic ironstones. Sediment. Geol. 372, 25–43.

Connelly, D.P., Statham, P.J., Knap, A.H., 2006. Seasonal changes in speciation of dissolved chromium in the surface Sargasso Sea. Deep-Sea Res. I Oceanogr. Res. Pap. 53, 1975–1988.

Cranston, R., Murray, J., 1978. The determination of chromium species in natural waters. Anal. Chim. Acta 99, 275–282.

Cranston, R., Murray, J., 1980. Chromium species in the Columbia River and estuary. Limnol. Oceanogr. 25, 1104–1112.

Crowe, S.A., Døssing, L.N., Beukes, N.J., Bau, M., Kruger, S.J., Frei, R., Canfield, D.E., 2013. Atmospheric oxygenation three billion years ago. Nature 501, 535–538.

D'Arcy, J., Babechuk, M.G., Døssing, L.N., Gaucher, C., Frei, R., 2016. Processes controlling the chromium isotopic composition of river water: constrains from basaltic river catchments. Geochim. Cosmochim. Acta 186, 296–315.

Dellwig, O., Beck, M., Lemke, A., Lunau, M., Kolditz, K., Schnetger, B., Brumsack, H.-J., 2007. Non-conservative behaviour of molybdenum in coastal waters: coupling geochemical, biological, and sedimentological processes. Geochim. Cosmochim. Acta 71, 2745–2761.

Dodson, M., 1963. A theoretical study of the use of internal standards for precise isotopic analysis by the surface ionization technique: part I-General first-order algebraic solutions. J. Sci. Instrum. 40, 289.

Dolamore-Frank, J.A., 1984. The Analysis, Occurrence and Chemical Speciation of Zinc and Chromium in Natural Waters. Ph.D. Thesis. University of Southampton, UK.

Døssing, L., Dideriksen, K., Stipp, S., Frei, R., 2011. Reduction of hexavalent chromium by ferrous iron: a process of chromium isotope fractionation and its relevance to natural environments. Chem. Geol. 285, 157–166.

Douglas, T.A., Chamberlain, C.P., Blum, J.D., 2002. Land use and geologic controls on the major elemental and isotopic (δ15N and 87Sr/86Sr) geochemistry of the Connecticut River watershed, USA. Chem. Geol. 189, 19–34.

Eary, L.E., Rai, D., 1987. Kinetics of chromium (III) oxidation to chromium (VI) by reaction with manganese dioxide. Environ. Sci. Technol. 21, 1187–1193.

Economou-Eliopoulos, M., Frei, R., Megremi, I., 2016. Potential leaching of Cr (VI) from laterite mines and residues of metallurgical products (red mud and slag): an integrated approach. J. Geochem. Explor. 162, 40–49.

Elderfield, H., 1970. Chromium speciation in sea water. Earth Planet. Sci. Lett. 9, 10–16.

Ellis, A.S., Johnson, T.M., Bullen, T.D., 2002. Chromium isotopes and the fate of hexavalent chromium in the environment. Science 295, 2060.

Ellis, A.S., Johnson, T.M., Bullen, T.D., 2004. Using chromium stable isotope ratios to quantify Cr (VI) reduction: lack of sorption effects. Environ. Sci. Technol. 38, 3604–3607.

Farkaš, J., Chrastny, V., Novak, M., Cadkova, E., Pasava, J., Chakrabarti, R., Jacobsen, S.B., Ackerman, L., Bullen, T.D., 2013. Chromium isotope variations ($\delta^{53/52}Cr$) in mantle-derived sources and their weathering products: Implications for environmental studies and the evolution of $\delta^{53/52}Cr$ in the Earth's mantle over geologic time. Geochim. Cosmochim. Acta 123, 74–92.

Fendorf, S.E., Zasoski, R.J., 1992. Chromium (III) Oxidation by δ-MnO_2. 1. Characterization. Environ. Sci. Technol. 26, 79–85.

Frei, R., Gaucher, C., Poulton, S.W., Canfield, D.E., 2009. Fluctuations in Precambrian atmospheric oxygenation recorded by chromium isotopes. Nature 461, 250–253.

Frei, R., Poiré, D., Frei, K.M., 2014. Weathering on land and transport of chromium to the ocean in a subtropical region (Misiones, NW Argentina): a chromium stable isotope perspective. Chem. Geol. 381, 110–124.

Garvine, R.W., 1974. Physical features of the Connecticut River outflow during high

discharge. J. Geophys. Res. 79, 831–846.
Garvine, R.W., 1975. The distribution of salinity and temperature in the Connecticut River estuary. J. Geophys. Res. 80, 1176–1183.
Gibbs, R.J., 1977. Transport phases of transition metals in the Amazon and Yukon Rivers. Geol. Soc. Am. Bull. 88, 829–843.
Gilleaudeau, G., Frei, R., Kaufman, A., Kah, L., Azmy, K., Bartley, J., Chernyavskiy, P., Knoll, A., 2016. Oxygenation of the mid-Proterozoic atmosphere: clues from chromium isotopes in carbonates. Geochem. Perspect. Lett. 2, 178–187.
Gordon, R.B., 1980. The sedimentary system of Long Island Sound. In: Advances in Geophysics. Vol. 22. Elsevier, pp. 1–39.
Goring-Harford, H.J., Klar, J., Pearce, C.R., Connelly, D.P., Achterberg, E.P., James, R.H., 2018. Behaviour of chromium isotopes in the eastern sub-tropical Atlantic Oxygen Minimum Zone. Geochim. Cosmochim. Acta 236, 41–59.
Gueguen, B., Reinhard, C.T., Algeo, T.J., Peterson, L.C., Nielsen, S.G., Wang, X., Rowe, H., Planavsky, N.J., 2016. The chromium isotope composition of reducing and oxic marine sediments. Geochim. Cosmochim. Acta 184, 1–19.
Holmden, C., Jacobson, A., Sageman, B., Hurtgen, M., 2016. Response of the Cr isotope proxy to cretaceous Ocean Anoxic Event 2 in a pelagic carbonate succession from the Western Interior Seaway. Geochim. Cosmochim. Acta 186, 277–295.
Hug, S.J., Laubscher, H.-U., James, B.R., 1996. Iron (III) catalyzed photochemical reduction of chromium (VI) by oxalate and citrate in aqueous solutions. Environ. Sci. Technol. 31, 160–170.
Jahns, R.H., 1947. Geologic Features of the Connecticut Valley, Massachusetts as Related to Recent Floods.
Jeandel, C., Minster, J.-F., 1984. Isotope dilution measurement of inorganic chromium (III) and total chromium in seawater. Mar. Chem. 14, 347–364.
Jeandel, C., Minster, J., 1987. Chromium behavior in the ocean: global versus regional processes. Glob. Biogeochem. Cycles 1, 131–154.
Kitchen, J.W., Johnson, T.M., Bullen, T.D., Zhu, J., Raddatz, A., 2012. Chromium isotope fractionation factors for reduction of Cr(VI) by aqueous Fe(II) and organic molecules. Geochim. Cosmochim. Acta 89, 190–201.
Kotaś, J., Stasicka, Z., 2000. Chromium occurrence in the environment and methods of its speciation. Environ. Pollut. 107, 263–283.
Mayer, L.M., Schick, L.L., Chang, C.A., 1984. Incorporation of trivalent chromium into riverine and estuarine colloidal material. Geochim. Cosmochim. Acta 48, 1717–1722.
McClain, C., Maher, K., 2016. Chromium fluxes and speciation in ultramafic catchments and global rivers. Chem. Geol. 426, 135–157.
Mugo, R.K., Orians, K.J., 1993. Seagoing method for the determination of chromium (III) and total chromium in sea water by electron-capture detection gas chromatography. Anal. Chim. Acta 271, 1–9.
Murray, J.W., Spell, B., Paul, B., 1983. The Contrasting Geochemistry of Manganese and Chromium in the Eastern tropical Pacific Ocean, Trace Metals in Sea Water. Springer, pp. 643–669.
Noordmann, J., Weyer, S., Montoya-Pino, C., Dellwig, O., Neubert, N., Eckert, S., Paetzel, M., Böttcher, M., 2015. Uranium and molybdenum isotope systematics in modern euxinic basins: case studies from the Central Baltic Sea and the Kyllaren fjord (Norway). Chem. Geol. 396, 182–195.
Novak, M., Chrastny, V., Čadková, E., Farkas, J., Bullen, T., Tylcer, J., Szurmanova, Z., Cron, M., Prechova, E., Curik, J., 2014. Common occurrence of a positive δ53Cr shift in Central European waters contaminated by geogenic/industrial chromium relative to source values. Environ. Sci. Technol. 48, 6089–6096.
Orians, K.J., Boyle, E.A., Bruland, K.W., 1990. Dissolved titanium in the open ocean. Nature 348, 322.
Paulukat, C., Døssing, L.N., Mondal, S.K., Voegelin, A.R., Frei, R., 2015. Oxidative release of chromium from Archean ultramafic rocks, its transport and environmental impact–a Cr isotope perspective on the Sukinda Valley ore district (Orissa, India). Appl. Geochem. 59, 125–138.
Paulukat, C., Gilleaudeau, G.J., Chernyavskiy, P., Frei, R., 2016. The Cr-isotope signature of surface seawater—a global perspective. Chem. Geol. 444, 101–109.
Pereira, N.S., Vögelin, A.R., Paulukat, C., Sial, A.N., Ferreira, V.P., Frei, R., 2015. Chromium isotope signatures in scleractinian corals from the Rocas Atoll, Tropical South Atlantic. Geobiology 4, 1–13.
Pettine, M., Millero, F.J., 1990. Chromium speciation in seawater: the probable role of hydrogen peroxide. Limnol. Oceanogr. 35, 730–736.
Pettine, M., Camusso, M., Martinotti, W., 1992. Dissolved and particulate transport of arsenic and chromium in the Po River (Italy). Sci. Total Environ. 119, 253–280.
Pfeiffer, W., Fiszman, M., de Lacerda, L.D., Van Weerelt, M., Carbonell, N., 1982. Chromium in water, suspended particles, sediments and biota in the Irajá river estuary. Environ. Pollut. B. 4, 193–205.
Planavsky, N.J., Reinhard, C.T., Wang, X., Thomson, D., McGoldrick, P., Rainbird, R.H., Johnson, T., Fischer, W.W., Lyons, T.W., 2014. Low Mid-Proterozoic atmospheric oxygen levels and the delayed rise of animals. Science 346, 635–638.
Rai, D., Eary, L., Zachara, J., 1989. Environmental chemistry of chromium. Sci. Total Environ. 86, 15–23.
Reinhard, C.T., Planavsky, N.J., Robbins, L.J., Partin, C.A., Gill, B.C., Lalonde, S.V., Bekker, A., Konhauser, K.O., Lyons, T.W., 2013. Proterozoic ocean redox and biogeochemical stasis. Proc. Natl. Acad. Sci. 110, 5357–5362.
Reinhard, C.T., Planavsky, N.J., Wang, X., Fischer, W.W., Johnson, T.M., Lyons, T.W., 2014. The isotopic composition of authigenic chromium in anoxic marine sediments: a case study from the Cariaco Basin. Earth Planet. Sci. Lett. 407, 9–18.
Richard, F.C., Bourg, A.C., 1991. Aqueous geochemistry of chromium: a review. Water Res. 25, 807–816.
Rotaru, M., Birck, J.L., Allegre, C.J., 1992. Clues to early solar system history from chromium isotopes in carbonaceous chondrites. Nature 358, 465–470.
Rudnick, R.L., Gao, S., 2003. Composition of the continental crust. In: Turekian, K., Holland, H.D. (Eds.), Treatise on Geochemistry. 3. Pergamon, Oxford, pp. 1–64.
Rue, E.L., Smith, G.J., Cutter, G.A., Bruland, K.W., 1997. The response of trace element redox couples to suboxic conditions in the water column. Deep-Sea Res. I Oceanogr. Res. Pap. 44, 113–134.
Saad, E.M., Wang, X., Planavsky, N.J., Reinhard, C.T., Tang, Y., 2017. Redox-independent chromium isotope fractionation induced by ligand-promoted dissolution. Nat. Commun. 8, 1590.
Schauble, E., Rossman, G.R., Taylor Jr., H.P., 2004. Theoretical estimates of equilibrium chromium-isotope fractionations. Chem. Geol. 205, 99–114.
Scheiderich, K., Amini, M., Holmden, C., Francois, R., 2015. Global variability of chromium isotopes in seawater demonstrated by Pacific, Atlantic, and Arctic Ocean samples. Earth Planet. Sci. Lett. 423, 87–97.
Schoenberg, R., Zink, S., Staubwasser, M., von Blanckenburg, F., 2008. The stable Cr isotope inventory of solid Earth reservoirs determined by double spike MC-ICP-MS. Chem. Geol. 249, 294–306.
Semeniuk, D., Maldonado, M.T., Jaccard, S.L., 2016. Chromium uptake and adsorption in cultured marine phytoplankton-implications for the marine Cr cycle. Geochim. Cosmochim. Acta 184, 41–54.
Shen, J., Liu, J., Qin, L., Wang, S.J., Li, S., Xia, J., Ke, S., Yang, J., 2015. Chromium isotope signature during continental crust subduction recorded in metamorphic rocks. Geochem. Geophys. Geosyst. 16.
Sirinawin, W., Turner, D.R., Westerlund, S., 2000. Chromium (VI) distributions in the Arctic and the Atlantic Oceans and a reassessment of the oceanic Cr cycle. Mar. Chem. 71, 265–282.
Smith, D.B., Cannon, W.F., Woodruff, L.G., Solano, F., Ellefsen, K.J., 2014. Geochemical and Mineralogical Maps for Soils of the Conterminous United States. (Seiries Editor).
USGS, 2003. U.S. Department of the Interior, Water Resources Information. http://www.usgs.gov/index/html.
Wang, X.L., Johnson, T.M., Ellis, A.S., 2015. Equilibrium isotopic fractionation and isotopic exchange kinetics between Cr (III) and Cr (VI). Geochim. Cosmochim. Acta 153, 72–90.
Wang, X.L., Planavsky, N., Hull, P., Tripati, A., Reinhard, C., Zou, H., Elder, L., Henehan, M., 2016a. Chromium isotopic composition of core-top planktonic foraminifera. Geobiology 1–14.
Wang, X.L., Planavsky, N.J., Reinhard, C.T., Zou, H., Ague, J.J., Wu, Y., Gill, B.C., Schwarzenbach, E.M., Peucker-Ehrenbrink, B., 2016b. Chromium isotope fractionation during subduction-related metamorphism, black shale weathering, and hydrothermal alteration. Chem. Geol. 429, 19–33.
Wang, X.L., Reinhard, C., Planavsky, N., Owens, J.D., Lyons, T., Johnson, C.M., 2016c. Sedimentary chromium isotopic compositions across the cretaceous OAE2 at Demerara Rise Site 1258. Chem. Geol. 429, 85–92.
Whitfield, M., 1987. The role of particles in regulating the composition of seawater. Aquat. Surf. Chem. 457–493.
Wu, W., Wang, X., Reinhard, C.T., Planavsky, N.J., 2017. Chromium isotope systematics in the Connecticut River. Chem. Geol. 456, 98–111.
Zink, S., Schoenberg, R., Staubwasser, M., 2010. Isotopic fractionation and reaction kinetics between Cr(III) and Cr(VI) in aqueous media. Geochim. Cosmochim. Acta 74, 5729–5745.